**Light Metals 2013** *Edited by: Barry Sadler*
***TMS (The Minerals, Metals & Materials Society), 2013***

# Light Metals 2013

## ALUMINUM REDUCTION TECHNOLOGY

## Fundamentals: Modelling

*SESSION CHAIR*
**Christian Droste**
Hydro Aluminium
Neuss, Germany

**Light Metals 2013** *Edited by: Barry Sadler*
***TMS (The Minerals, Metals & Materials Society), 2013***

# Unsteady MHD modeling applied to cell stability

RENAUDIER Steeve[1]; BARDET Benoit[1]; STEINER Gilles[2]; PEDCENKO Alex[3]; RAPPAZ Jacques[4]; MOLOKOV Sergeï[3]; MASSEREY Alexandre[2]
[1]Rio Tinto Alcan – LRF ; Saint-Jean-de-Maurienne 73303 ; BP 114 – Cedex ; France;
[2]Ycoor Systems SA; Sierre 3960; Technopôle 10 ; Switzerland;
[3]Coventry University; Faculty of engineering and computing - MCE; Priory Street; CV15FB; United Kingdom;
[4]EPFL-SB-IACS; Lausanne CH-1015; Station 8; Switzerland;

Keywords: energy consumption, MHD, stability, ACD

## Abstract

In a context of higher energy prices, reducing energy consumption is a top priority for any new technological development. One of the main levers is to reduce Anode to Cathode Distance (ACD), but doing so directly increases Magneto-Hydro-Dynamic (MHD) instabilities and thereby reduces current efficiency. To limit MHD instabilities, Rio Tinto Alcan has carried out an extensive modeling and experimental program with the support of EPFL (Ecole Polytechnique Fédérale de Lausanne) and Coventry University. This article compares the results obtained using the latest unsteady stability model, developed by EPFL, with the lab-scale Coventry experiment and with industrial AP3X operating results. This new model clearly provides a good prediction of instability when metal height and ACD are reduced, at both lab and industrial scales. It overcomes the limitations of the usual shallow-water or linear stability models, for which extensive assumptions have to be made. It opens broad possibilities for investigating new solutions to reduce MHD instabilities.

## Introduction

MHD instabilities within electrolysis cells

Figure 1 shows a schematic representation of the steady state of an electrolysis cell. The current flows from the anode, crossing the electrolyte and the liquid aluminum layers, and exits at the cathode. The high amperage creates a large magnetic field, which generates flow within the cell. Under certain conditions, the bath-metal interface can become unstable, degrading the efficiency of the process.

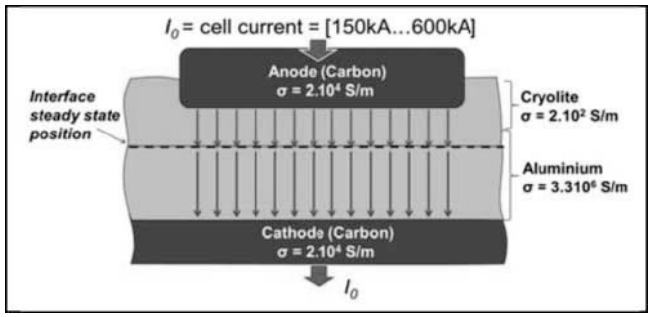


*Fig.1: Steady state position of the interface*

The bath-metal interface of an electrolysis cell is continuously subjected to perturbations, the smallest ones being the release of gas bubbles and the largest ones tapping or anode changes. Due to the differences in electric conductivity (σ) between the electrolyte and the aluminum, a perturbation can lead to major current redistribution within the cell, as illustrated on figure 2.

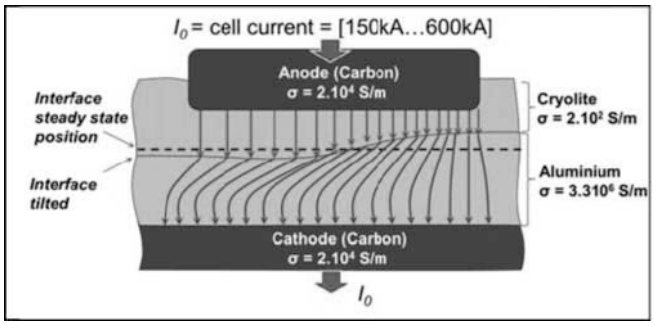


*Fig.2: Perturbation of the interface*

Figure 3 represents a tilted interface. It can be shown that the perturbed currents are horizontal in the metal. Through interaction with the vertical component of the magnetic field ($B_{z0}$), this generates a horizontal MHD force. The perturbation is then transported by this force until it is reflected on the cell borders. According to Sele's criterion β [1], depending on the $B_{z0}$, $I_0$, ACD and $H_{Al}$ values, the perturbation can be either stabilized or amplified. ACD, $H_{Al}$ and $I_0$ are operating parameters while the $B_{z0}$ depends on the cell design.

Indeed, it is important to point out that the $B_{z0}$ is due mainly to the cell busbar arrangement. The current is transported by busbars from one pot to the next. The path taken by the busbars provides the intensity and distribution of $B_{z0}$ within the cell. To summarize, busbar design imposes the overall magnetic configuration of a cell, which is at the core of the issue of cell instability and process efficiency.

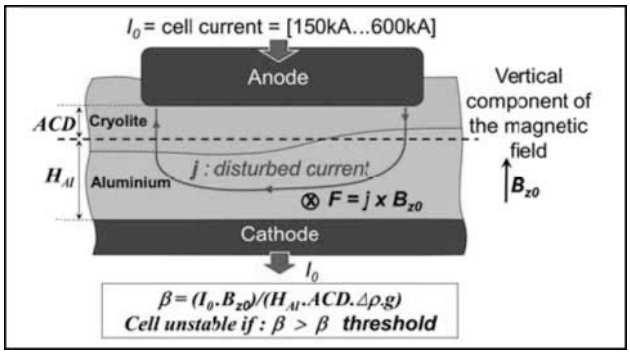


*Fig.3: Interaction of disturbed current with vertical component of magnetic field*

The common technological challenge for primary aluminum producers is to minimize ACD in order to reduce energy consumption, with the highest current density in order to

maximize productivity. However, these two operating parameters increase MHD instabilities, thereby reducing process efficiency. Finally, it is widely known that the most reliable way to ensure a stable cell is to optimize its magnetic design, which depends on its busbar design.

Overview of existing models

After Sele's model [1], several other models of different levels of complexity have been proposed in order to account for cell dimensions, horizontal currents and the three components of the magnetic field (cf. [2] to [12]). However, even the more complex models, such as shallow water and linear stability models, still require geometrical assumptions.

In practice, these models are efficient in performing incremental studies from a reference case. However, if the new cell modeled has different dimensions to those of the reference case, combined with a new magnetic field balance, then the stability prediction of any existing model will not be accurate enough to determine what ACD savings can be obtained. Furthermore, considering the very good performance of Rio Tinto Alcan's benchmark technologies in terms of MHD stability and ACD squeezing potential, model results will have to be accurate enough to ensure and quantify stability improvements compared to the best existing technologies.

In the framework of a technology step-change study, the application fields and the level of accuracy of existing models become too limited. Moreover, the level of accuracy required for modeling results has drastically increased as the majority of Rio Tinto Alcan smelters have considerably squeezed their pots. ACD values are becoming very small, thus increasing the numerical difficulty of capturing instabilities. It is for this reason that the 3D unsteady stability model presented in this paper was developed.

3D unsteady stability model and MHD experiment

In order to maximize its chances of success when designing a new cell technology, Rio Tinto Alcan carried out an extensive MHD modeling and experimental program over a period of many years. The final objective of this program was to develop and validate a 3D nonlinear unsteady model that fully solves fluid flow equations with a moving interface. This model was developed by EPFL, and its performance was then optimized by Ycoor Systems. Rio Tinto Alcan then used and validated it.

A full 3D nonlinear unsteady model was proposed for the first time in [13]. However, the solving methods were too demanding in terms of CPU time to model MHD on a real cell. This first 3D nonlinear unsteady model was limited to academic cases. Now, with the 3D nonlinear unsteady model presented in this paper, a real cell can be modeled with an acceptable CPU time.

In parallel, an experiment was performed at Coventry University [14]. This experiment provided further fundamental understanding of MHD instabilities but also very accurate experimental data for model validation.

**Unsteady stability model developed by EPFL**

Model presentation

Figure 4 presents the model geometry, in this case that of a P155 cell. All the conducting parts of the cell are meshed in order to compute precisely the current distribution in the conductors and then the magnetic field. The potshell is also meshed in order to model its ferromagnetic impact on the magnetic field within the liquids. It is important to note that all surrounding conductors generating a magnetic field, that do not belong to the pot to pot busbar circuit, are also modeled. The closest neighboring pots are duplicated in order to account for their magnetic impact.

All variables are calculated on the same mesh using finite-element methods. The mesh was optimized in order to provide reliable results with an acceptable CPU time.

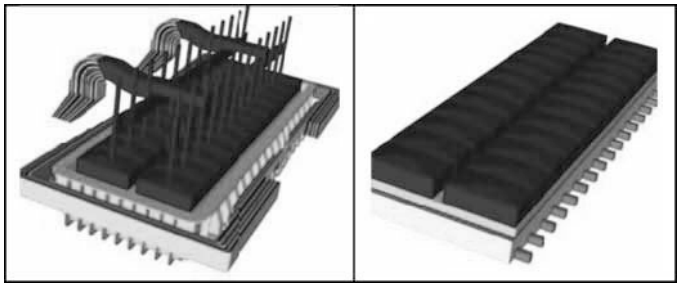

*Fig. 4: On the left, view of a full cell modeled; on the right, view of this cell without potshell, busbars and anode rods.*

Figure 5 presents a macro description of the 3D nonlinear unsteady model algorithm. Once the mesh is generated, material properties defined and boundary conditions imposed, the simulation starts by computing the electric potential distribution within the cell. The current density in the whole cell is then deduced and the magnetic field is calculated by using the Biot and Savart law. Once the magnetic field is known, the ferromagnetism of the potshell is calculated in order to obtain the induction distribution within the liquids and hence the Lorentz force. Given the Lorentz force distribution in the liquids, the velocity field can be calculated by solving the three-dimensional Navier-Stokes equations. At the first time iteration, a flat interface is assumed.

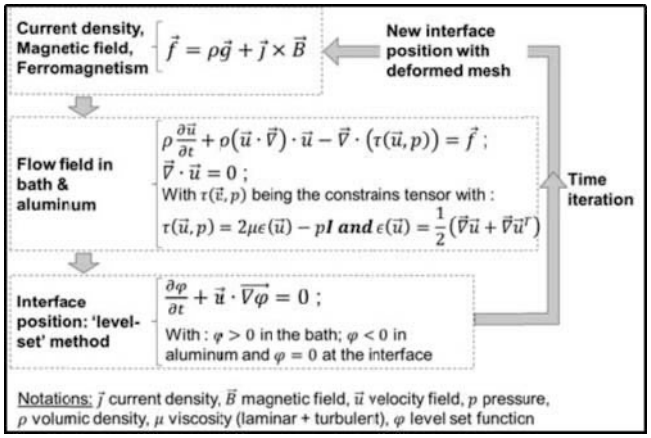


*Fig. 5: Macro description of the unsteady model*

Once the velocity field has been calculated, the interface position is recomputed in order to fulfill the continuity of the tangential velocities through the interface and the condition of fluid immiscibility (normal component of velocity must be zero at the interface). Numerically, the interface position is calculated using a level-set method. Once the new position of the interface is determined, the mesh in the liquids is deformed (cf. figure 6) in order to place interface nodes at the new positions calculated by the level-set method.

For the next time step, the previously calculated interface position leads to a modification in the electrical potential distribution. Electrical potential is therefore calculated at the beginning of the next time step and the Lorentz forces are updated using the new current density value. Then, as described previously for the first time iteration, the velocity field and the new interface position are recomputed.

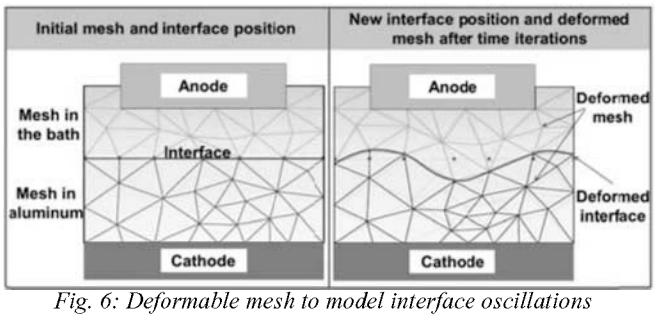


*Fig. 6: Deformable mesh to model interface oscillations*

Anodic plane

It is important to mention that preliminary initialization of the anodic plane is required before starting the full unsteady simulations. Indeed, on a real cell the anodic plane is consumed so that the ACD remains constant. The shape of the anodic plane is therefore roughly the same as that of the interface. Numerically, a preliminary calculation is performed to determine the "average steady state" position of the interface. It is from this interface position, with an anodic plane deformed in such a way that the ACD is constant, that the unsteady simulations are started.

Interpretation of results

The unsteady model computes time-dependent oscillations of the interface and all variables are calculated at each time step on each mesh element. However, in order to compare the model results with those obtained during actual operation, the only reliable variable measured on a real cell is its overall voltage drop. From this variable, the instability level is determined by calculating voltage drop fluctuations each minute.

In the next part of this paper we will present the results obtained during the Coventry experiment, in which it was possible to directly observe the interface oscillations and detect the stability threshold. We will then present the results obtained on AP3X cells when the ACD was reduced. For these results we compared the measured voltage drop fluctuations with those predicted by the model.

**The Coventry experiment for MHD instabilities: comparison with modeling results**

Presentation of the experiment

The experimental set-up (figure 7) comprises a rectangular box of 30×30 cm2 horizontal cross-section with an electrically conducting top and bottom and non-conducting, 15 cm high side walls. The box is partially filled with liquid metal, an In-Ga-Sn alloy. A DC electric current is supplied from the top of the container (anode plate) to the bottom (cathode plate) through the liquid metal layer. On figure 7, the electrolyte layer, which is normally located above the aluminum layer in industrial cells, is replaced by a system of vertical electrodes immersed in water and dipped vertically 1mm into the liquid metal.

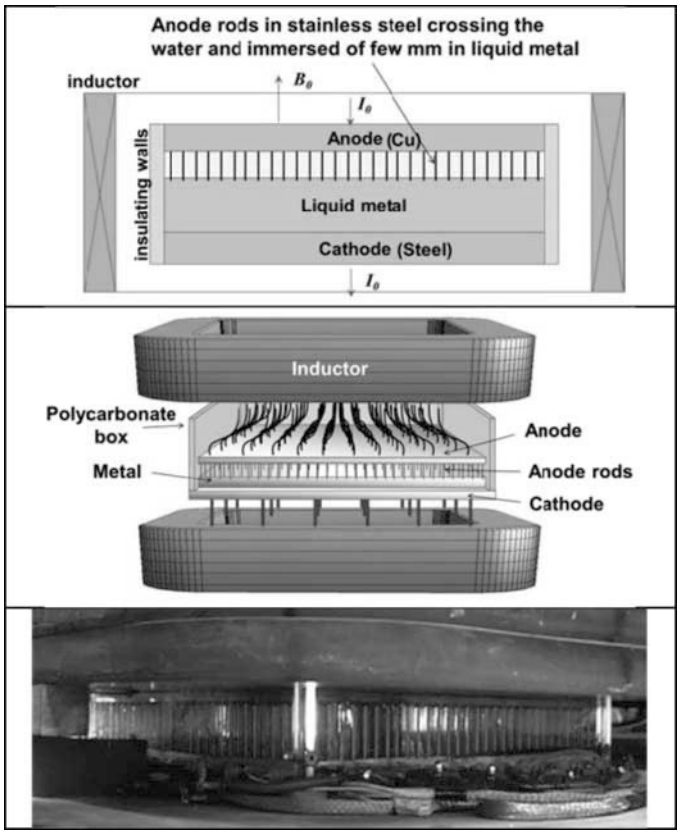


*Fig.7 Presentation of the Coventry MHD experiment*

The electrodynamic properties of this type of multi-electrode structure are similar to those of the electrolyte layer in the industrial cell: this establishes sufficient uniformity of the vertical current along the free surface of the liquid metal if it is undisturbed. On figure 8, it can be seen that if the liquid metal surface is deformed, it amplifies the current in the deeper liquid metal areas and lowers it in the shallow ones. The disturbed currents that appear are very similar to those encountered on a real cell.

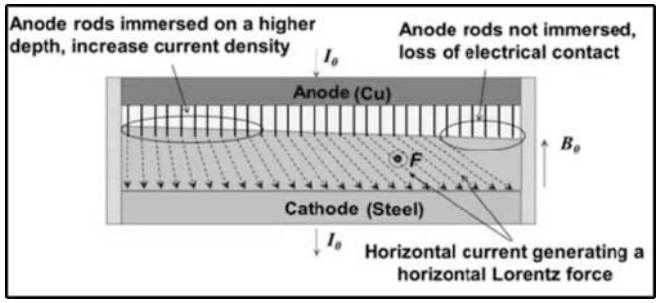


*Fig.8 Generation of disturbed current on the Coventry experiment*

The use of 'multi-electrode' anodes as a replacement for an electrolyte layer eliminates many undesired side-effects: electrolysis, high Joule heat losses in the electrolyte, ionic conductivity, high temperatures, need for electrolyte cooling and continuous renewal, high chemical aggressiveness of the media, need to remove electrolysis products including gases, etc. In contrast, a multi-electrode 'electrolyte model' is safe, enables a vertical current of up to 2 kA to be used, is at room temperature, and consumes little electric power.

The cell with the liquid metal was placed in the vertical, uniform, steady magnetic field generated by rectangular water-cooled Helmholtz coils (cf. figure 7), fed with DC current from two other 600A current sources, which provide maximum density of the ~100 mT magnetic flux and ~5% maximum non-uniformity of the field's vertical component in the liquid metal volume.

This experimental set-up captures the stability threshold very precisely. In practice, the experiment is performed by fixing a magnetic field value, then the current is strongly increased until the interface becomes unstable. The amperage is then decreased until the wave is damped. The transition between a stable and an unstable case is very clear in the range of only few amperes. The stability thresholds obtained with this facility are accurate and reproducible.

Experimental modeling

The experiment simulated the area from the upper part of the anode to the lower part of the cathode, which consisted in meshing a very simple square box with two solid plates and two immiscible liquids. The main problem involved modeling the anode rods. Taking into account the large number of anode rods (900) and their small size, it was not possible to mesh each anode rod in order to avoid excessively long CPU time. Furthermore the only limitation of the unsteady model is that the interface must keep the same topology, which means it is impossible to model the moment when an anode rod loses contact with the interface.

In order to overcome this problem of anode rod representation, only the electrical impact of the anode was represented. A bath electrical conductivity value equivalent to the one including anode rods plus bath was defined in the model. Finally, to represent the loss of contact between interface and anode rods, a variable conductivity value was defined in the modeled bath. When the position of the interface is lower than the immersion depth, the loss of electrode contact is represented by imposing a very low conductivity value in the bath area between the bottom of the electrodes and the interface position (cf. figure 8).

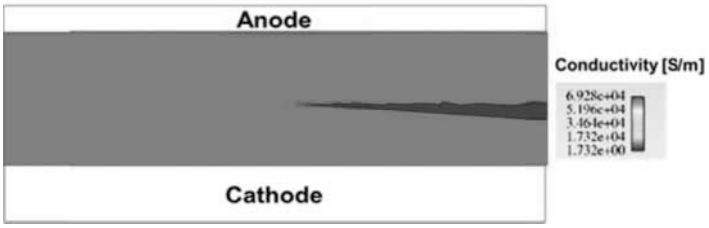


*Fig. 8: Electrical conductivity in the liquids: loss of electrical contact when interface is lower than anode rods.*

Figure 9 represents the electric potential distribution superimposed with current density vectors in order to show that the loss of electrical contact of the anode rods generates a high horizontal current in the cell. This loss of electrical contact strongly amplifies the MHD destabilization impact and as the depth of immersion is very small (about 1 mm), the stability threshold can be capture very precisely.

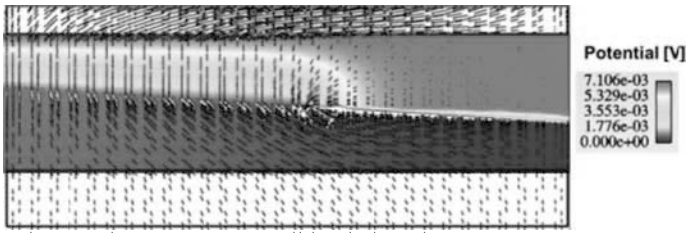


*Fig. 9: Electric potential and current density vectors*

Modeling vs. experimental results

Figure 10 superimposes the experimental and modeling results in terms of stability threshold, for a metal height of 35 mm and immersed anode depth of 1 mm. The "stability threshold" is the minimum values of B and I for the instability to survive. Below these values, instabilities become negligible. Figure 10 clearly shows the very good agreement obtained between the experimental and modeling results.

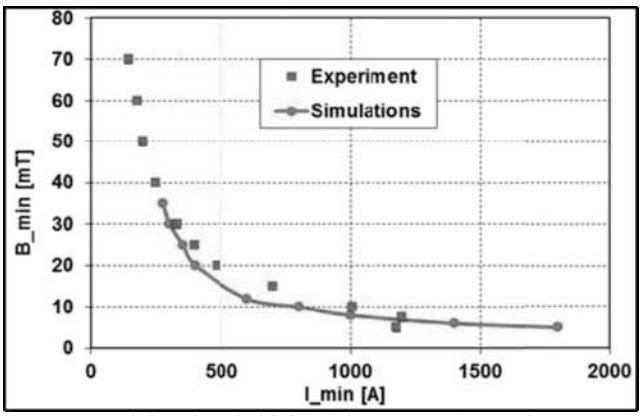


*Fig. 10: Stability threshold depending on B0 (vertical magnetic field) and I (current), comparison between experiment and simulations.*

In order to illustrate the sensitivity of the stability threshold, figure 11 plots the modeling results for the time-dependent change in electrical potential of the cell (scaled by the initial value). Amperage is fixed at 600 A and three values of Bz (10, 12 and 15 mT) are represented. It can be seen clearly that the cases of 12 and

15 mT are unstable, and the case of 10 mT is stable. This means that the threshold is between 10 and 12mT, which is already a small interval of uncertainty. If required, additional simulations can then be performed in order to assess this threshold interval more precisely.

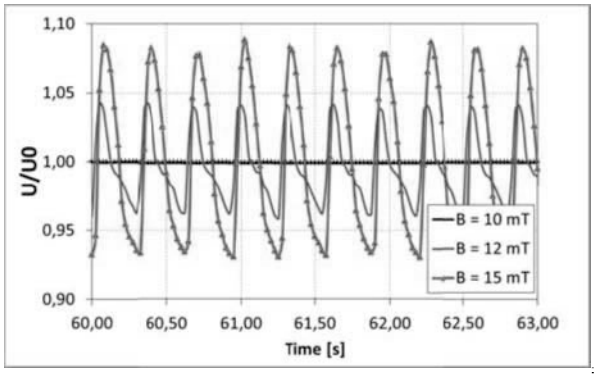


*Fig. 11: Relative cell voltage drop at 600 A.*

Figure 12 shows snapshots of the interface during a period of instability for a cell amperage of 1200 A and a Bz of 100 mT. The periods and shape of the interface are almost the same.

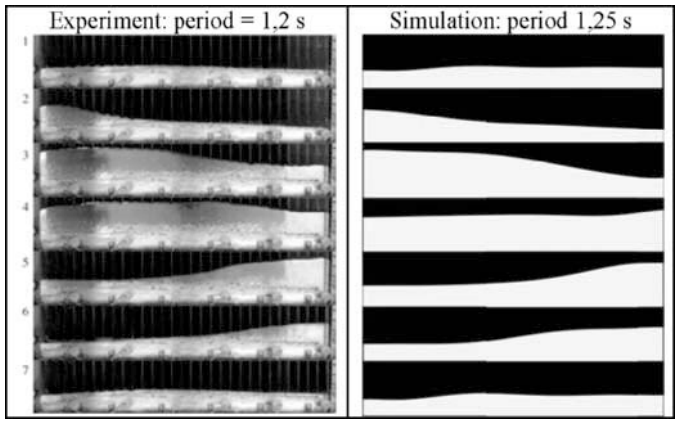


*Fig. 12: Experiment vs. simulations for 100 mT and 1200 A*

The average deviation of the interface from its initial position ("STDev") or the average absolute amplitude has been plotted on figure 13 for Bz values of 20 and 50 mT depending on cell amperage. The curve trends are the same but the amplitudes obtained by the simulations are bigger for low amperages and smaller for high amperages. The differences at low amperages are probably due to the removal of anode rods. When the Lorentz force in the cell is weak, the breaking effect of the anode rods is relevant and will tend to damp instabilities. When Lorentz forces are higher (higher amperage), anode rod breaking effect becomes negligible and the resulting differences can be explained by the higher diffusivity of the model compared to reality.

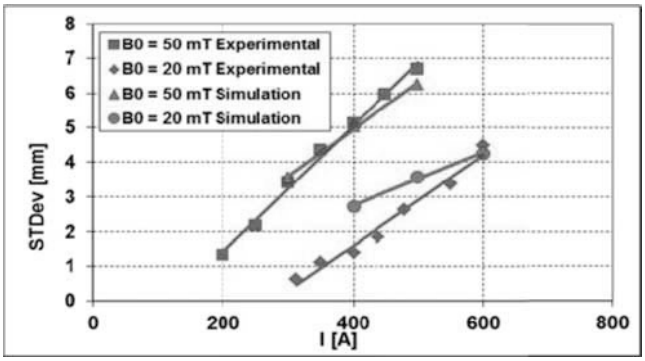


*Fig. 13: Standard deviation of interface depending on cell amperage and vertical magnetic field*

To conclude, with regard to the Coventry lab scale experiment, the modeling and experimental results appear to be in fairly good agreement in terms of stability predictions. The time-dependent changes in the interface obtained by the unsteady model are very similar to those observed on the facility. Some small differences remain in terms of amplitude but they are mainly due to the simplification in modeling anode rods.

**AP3X technology application: modeling results compared to smelter operating results**

The ultimate validation of the unsteady stability model was to perform simulations when reducing ACD. In contrast to the Coventry experiment, the calculations started by computing the "average steady state" providing average metal upheaval and flow field in the liquids. The anodic plane is eroded in such a way that ACD is constant. Figure 14 presents the average steady state interface and velocity field for the AP3X reference case. This steady state has to be recomputed for any new operating conditions. The unsteady calculation is then launched from this steady state.

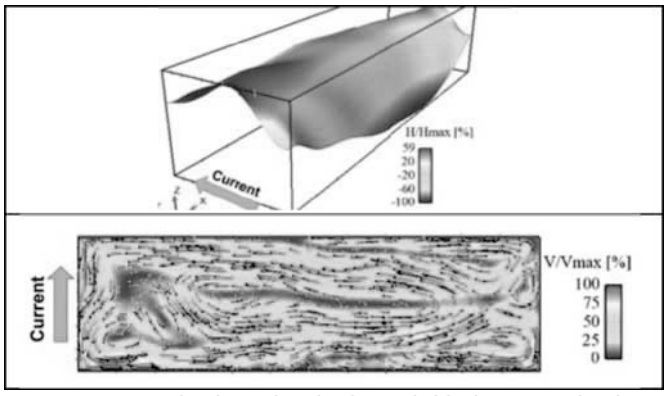


*Fig. 14: Metal upheaval and velocity field of an AP3X for the reference case*

Figure 15 shows time-dependent changes in the electric potential of the cell for different ACD values given as a percent of a reference value. It is clear that reducing the ACD increases fluctuations in potential, which is in agreement with the expected physical behavior. However, the goal of the model is to determine whether these potential fluctuations are in agreement with cell operating results.

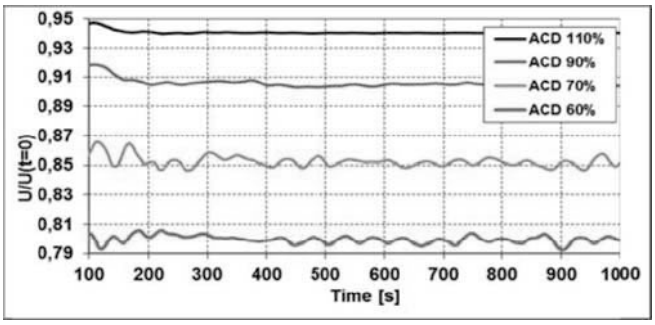


*Fig. 15: Time-dependent changes in electric potential for an AP3X scaled by the initial value at t=0*

Figure 16 compares the results of the unsteady model with those obtained during operation. The graph plots the fluctuations in electric potential averaged over intervals of one minute:

**Delta{U/U_ref} = Average over 60s(Max{U/Uref}-Min{U/Uref})**

Operating results were obtained from AP3X smelters by performing an extensive statistical analysis covering three years and one thousand cells. These results are represented on figure 16 by the blue area limited by the blue dotted curves.

Results directly obtained by the model are represented by the red curve. A significant difference between the operating results and modeling results can be observed but the trend is the same. The most important thing is that the increase in voltage drop fluctuations when ACD is reduced is correctly predicted. It is also important to note that both the experimental and modeling curves tend to flatten beyond 110% of baseline ACD. In the case of the operating results, there is a remaining steady noise that is not represented by our model. This remaining noise is due mainly to model assumptions concerning cell operations.

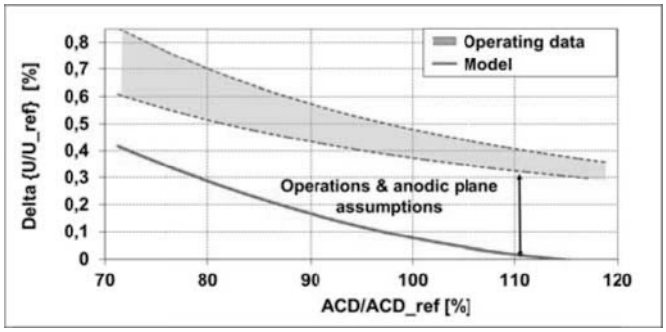


*Fig. 16: Comparison of cell voltage drop fluctuations when ACD is reduced: modeling results vs. operating results on AP3X*

Indeed, the cell is never in a steady state, in contrast to our modeling assumptions. The unsteady simulation starts from an average steady state in ideal operating conditions: all the anodes have the same conductivity (same temperature), and metal height is set at its nominal value. It is widely known and observed in practice that anode change or tapping operations considerably increase instability. These operations lead to a significant modification in current distribution within the cell. Metal upheaval is modified significantly as a consequence over a much shorter time scale than that required for the anodic plane to be eroded in such a way that ACD is constant.

To summarize, the model does not and cannot take into account the fact that the cell is always in a transitional state. As a consequence there are weak disturbed currents due to operations that will always remain in a real cell leading to instabilities and hence to voltage drop fluctuations. This is what explains the differences between the modeling and operating results and the fact that both curves tend to flatten on figure 16, with a limit at zero for the model and a constant for operating results. Finally, accounting for this constant difference due to operations that cannot be modeled, we can conclude that model results are in good agreement with operating ones.

## Conclusions

This paper presents the results of the latest unsteady stability model developed by EPFL. The results were compared with the Coventry lab scale experiment and with AP3X operating results when ACD is reduced. We have demonstrated that the results obtained are in fairly good agreement with the experimental results at both lab and industrial scales using the same numerical settings.

To conclude, the results presented in this paper show the ability of our model to treat any kind of cell dimensions and configurations without any extra numerical calibration. This model offers wide possibilities of application for precisely assessing the squeezing potential of technology step change design.

## Acknowledgements

First, we want to thank O. Martin for having sponsored and strengthened this MHD modeling and experimental program since 2005. Many thanks to T. Tomasino, who led the modeling team and the MHD program for many years. We also want to thank Y. Caratini, our modeling team leader and thermal expert, for his advice and for always making the link between MHD and cell thermal balance.

## References

[1] Sele, T.: Metallurgical Transactions 8B (1977) 613-618
[2] Urata, N.: Light Metals (1985) 581-591
[3] Lukyanov, A.; El, G.; Molokov, S.: Phys. Lett. A., 290 (2001) 165-172
[4] Molokov, S.; El, G.; Lukyanov, A.: Coventry University, AMRC Internal Report AM-01/2003 (2003)
[5] Kohno, H.; Molokov, S.: Phys Lett A 366 (2007) 600-605
[6] Kohno, H.; Molokov, S.: Int J Engng Sci 45 (2007) 644-659
[7] Sun, H.; Zikanov, O.; Ziegler, P.: Fluid Dynamics Research 35 (2004) 255–274
[8] Davidson, P.A.; Lindsay, R.L.: J. Fluid Mech 362 (1998) 273-295
[9] Bojarevics, V.; Romerio, M.V.: Eur. J Mech B/Fluids 13 (1994) 33-56
[10] Bojarevics, V.; Pericleous, K.: Light Metals (2006) 347-352
[11] Sneyd, A.D.: J Fluid Mech 236 (1992) 111-126
[12] Sneyd, A.D.; Wang, A.: J Fluid Mech 236 (1994) 111-126
[13] Gerbeau J.-F., Le Bris; C., Lelievre: T. Mathematical Methods for the Magnetohydrodynamics of Liquid Metals. Oxford University Press (2006)
[14] A. Pedchenko, S. Molokov, J. Priede, A. Lukyanov and P. J. Thomas. Experimental Model of the Interfacial Instability of Aluminium Reduction Cells. Europhysics Letters, vol.88, 2, 2009